THE JOURNAL OF BIOLOGICAL CHEMISTRY VOL. 285, NO. 41, pp. 31806–31818, October 8, 2010

Mechanism of Hyperinsulinism in Short-chain 3-Hydroxyacyl-CoA Dehydrogenase Deficiency Involves Activation of Glutamate Dehydrogenase*

Received for publication, March 15, 2010, and in revised form, July 1, 2010 Published, JBC Papers in Press, July 29, 2010, DOI 10.1074/jbc.M110.123638

Changhong Li,[a] Pan Chen,[a] Andrew Palladino,[a] Srinivas Narayan,[b] Laurie K. Russell,[c] Samir Sayed,[a] Guoxiang Xiong,[d] Jie Chen,[b] David Stokes,[a] Yasmeen M. Butt,[e] Patricia M. Jones,[e] Heather W. Collins,[f] Noam A. Cohen,[d] Akiva S. Cohen,[d] Itzhak Nissim,[g] Thomas J. Smith,[h] Arnold W. Strauss,[i] Franz M. Matschinsky,[f] Michael J. Bennett,[b] and Charles A. Stanley[a1]

From the [a]Division of Endocrinology and the [b]Department of Pathology and Laboratory Medicine, The Children's Hospital of Philadelphia, Philadelphia, Pennsylvania 19104, the [c]Department of Biology, Saint Louis University, St. Louis, Missouri 63103, the [d]Division of Neurology, The Children's Hospital of Philadelphia, Philadelphia, Pennsylvania 19104, [e]Children's Medical Center, University of Texas Southwestern Medical Center, Houston, Texas 75235, the [f]Department of Biochemistry and Biophysics, University of Pennsylvania School of Medicine, Philadelphia, Pennsylvania 19104, the [g]Division of Child Development and Pediatrics Rehabilitation, The Children's Hospital of Philadelphia, Philadelphia, Pennsylvania 19104, [h]Danforth Plant Research Institute, St. Louis, Missouri 63132, and the [i]Department of Pediatrics, University of Cincinnati College of Medicine, Cincinnati, Ohio 45229

The mechanism of insulin dysregulation in children with hyperinsulinism associated with inactivating mutations of short-chain 3-hydroxyacyl-CoA dehydrogenase (SCHAD) was examined in mice with a knock-out of the *hadh* gene (*hadh*$^{-/-}$). The *hadh*$^{-/-}$ mice had reduced levels of plasma glucose and elevated plasma insulin levels, similar to children with SCHAD deficiency. *hadh*$^{-/-}$ mice were hypersensitive to oral amino acid with decrease of glucose level and elevation of insulin. Hypersensitivity to oral amino acid in *hadh*$^{-/-}$ mice can be explained by abnormal insulin responses to a physiological mixture of amino acids and increased sensitivity to leucine stimulation in isolated perifused islets. Measurement of cytosolic calcium showed normal basal levels and abnormal responses to amino acids in *hadh*$^{-/-}$ islets. Leucine, glutamine, and alanine are responsible for amino acid hypersensitivity in islets. *hadh*$^{-/-}$ islets have lower intracellular glutamate and aspartate levels, and this decrease can be prevented by high glucose. *hadh*$^{-/-}$ islets also have increased [U-^{14}C]glutamine oxidation. In contrast, *hadh*$^{-/-}$ mice have similar glucose tolerance and insulin sensitivity compared with controls. Perifused *hadh*$^{-/-}$ islets showed no differences from controls in response to glucose-stimulated insulin secretion, even with addition of either a medium-chain fatty acid (octanoate) or a long-chain fatty acid (palmitate). Pull-down experiments with SCHAD, anti-SCHAD, or anti-GDH antibodies showed protein-protein interactions between SCHAD and GDH. GDH enzyme kinetics of *hadh*$^{-/-}$ islets showed an increase in GDH affinity for its substrate, α-ketoglutarate. These studies indicate that SCHAD deficiency causes hyperinsulinism by activation of GDH via loss of inhibitory regulation of GDH by SCHAD.

Congenital hyperinsulinism is the most common cause of persistent hypoglycemia in infants and children (1). Six genetic loci have been associated with the disorder. The most common of these disorders are due to inactivating mutations of the sulfonylurea receptor 1 (SUR1)[2] and Kir6.2 subunits of the β-cell ATP-dependent potassium (K_{ATP}) channel or to activating mutations of glutamate dehydrogenase (GDH) and glucokinase. Recently, several children have been described with a recessively inherited form of hyperinsulinism that is associated with deficiency of a mitochondrial fatty acid β-oxidation enzyme, short-chain 3-hydroxyacyl-CoA dehydrogenase (SCHAD) encoded by the *HADH* gene on 4q (2–4). SCHAD catalyzes the third step in the β-oxidation cycle for medium and short-chain 3-hydroxy fatty acyl-CoAs. Children afflicted with SCHAD deficiency have recurrent episodes of hypoglycemia that can be prevented by treatment with diazoxide (2, 3) and also have characteristic accumulations of fatty acid metabolites, including plasma 3-hydroxybutyrylcarnitine and urinary 3-hydroxyglutaric acid (2, 3). This form of abnormal insulin regulation is unique, because other genetic disorders of mitochondrial fatty acid oxidation do not cause hyperinsulinism (5). In addition, the genetic defect in SCHAD deficiency is expected to impair, rather than increase, the production of ATP, which normally serves as the triggering signal for insulin release. An important clue to the mechanism of insulin dysregulation in SCHAD deficiency has been recently provided by the report

* This work was supported, in whole or in part, by National Institutes of Health Grants DK53012 (to C. A. S.), DK22122 (to F. M. M.), DK 53761 (to I. N.), HL075421 (to A. W. S.). This work was also supported by a fellowship award from Society for Inherited Metabolic Disorders (to A. P.). Additional support was provided by the Radioimmunoassay and Islet Cores of the Diabetes Research Center of the University of Pennsylvania School of Medicine (Grant DK19525) and Clinical & Translational Research Center (UL1-RR-024134). The work was presented in part at the annual meeting of Society for Inherited Metabolic Disorder (March 25–28, 2007, Nashville, Tennessee) and 69th annual meeting of American Diabetes Association (June 5–9, 2009, New Orleans).

[1] To whom correspondence should be addressed: Division of Endocrinology, The Children's Hospital of Philadelphia, 34th St. and Civic Center Blvd., Philadelphia, PA 19104. Tel.: 215-590-3420; Fax: 215-590-1605; E-mail: stanleyc@email.chop.edu.

[2] The abbreviations used are: SUR1, sulfonylurea receptor 1; SCHAD, short-chain 3-hydroxyacyl-CoA dehydrogenase; GDH, glutamate dehydrogenase; GSIS, glucose-stimulated insulin secretion; $[Ca^{2+}]_i$, cytosolic calcium; ES, embryonic stem cell; AAM, amino acid mixture.

that affected children are sensitive to protein-induced hypoglycemia (6).

Elucidating the mechanism of insulin dysregulation and, especially, the cause of the hypersensitivity to protein-induced hypoglycemia in SCHAD deficiency may provide important insight into the regulation of insulin secretion in normal individuals. The present report describes studies of a mouse model of SCHAD deficiency that was developed by ablation of the mouse *hadh* gene. The results suggest that the dysregulation of insulin secretion associated with SCHAD deficiency is due to an activation of GDH enzyme activity, reflecting the loss of an inhibitory protein-protein interaction of SCHAD upon GDH, which has not previously been recognized.

EXPERIMENTAL PROCEDURES

SCHAD (hadh) Gene Targeting—$hadh^{-/-}$ mice were generated by homologous recombination in R1 mouse embryonic stem (ES) cells. Genomic DNA corresponding to the Sv129/J mouse *hadh* gene was isolated in overlapping bacteriophage lambda clones (Stratagene) and a P1 clone (Incyte Genomics, Palo Alto, CA), and the nucleotide sequences of the exons and flanking intronic sequences were determined. The knock-out targeting vector was constructed in the pPNT vector. A 4.2-kb fragment from immediately upstream of exon 1 and a 0.8-kb PstI fragment from downstream of exon 1 of the *hadh* gene were used to flank the neomycin resistance cassette in the targeting construct. The linearized targeting construct was electroporated into R1 ES cells, and the ES cells were subjected to positive and negative selection with G418 (250 μg/ml, Invitrogen) and 2-deoxy-2-fluoro-β-D-arabinofuranosyl)-5-iodouracil, respectively. Ninety-five clones survived selection and were subsequently screened by a PCR assay to identify homologous recombinants (primer sequences and PCR conditions are available upon request). One homologous recombinant was detected and confirmed by Southern blotting. The clonal *hadh* knock-out ES cell line was injected into C57/BL6 blastocysts followed by implantation into pseudo-pregnant female mice to generate chimeras. High percentage (~80%) male chimeras were bred to NIH Black Swiss females to generate $hadh^{+/-}$ heterozygotes.

Mouse Breeding and Genotyping—Deletion of *hadh* did not affect intrauterine or post-natal growth or survival. Knock-out and control mice had similar body weights and growth rates (data not shown). Mouse genotyping was performed by PCR: the primer sequences were 5′-CAC TGA GCTATG GCG TTC GTG AAC A-3′ and 5′-TCT GCA ACT TTG CAC GCA CAA CTG TGT-3′ for $hadh^{+/+}$, and 5′-AAT CAG CAG TGA GAG AGC CAC AGG CAA-3′ and 5′-TGC TAA AGC GCA TGC TCA CAG ACT GC-3′ for $hadh^{-/-}$. The PCR assay generated products of 359 bp for the wild-type *hadh* allele and 800 bp for the *hadh* knock-out allele.

RT-PCR and Western Blot Analysis—For RT-PCR analysis, total RNA was isolated from fresh tissue, including pancreatic islets, liver, kidney, and brain using TRIzol (Invitrogen). cDNA was generated by reverse transcription using a Superscript First Strand Kit (Invitrogen). The sequences of primers for PCR amplification of *hadh* and GAPDH mRNA were: for *hadh*-forward, 5′-CCA CCA GAC AAG ACC GAT-3′; for *hadh*-reverse, 5′-TCA ATG AGG TAT GGC ACC AA-3′; for GAPDH-forward, AAC TTT GGC ATT GTG GAA GG-3′; and for GAPDH-reverse, GGA TGC AGG GAT GAT GTT CT-3′. PCR products of 208 bp for *hadh* and 132 bp for GAPDH were generated.

Western blots were performed on whole tissue protein extracts (pancreatic islets, liver, kidney, and brain) to detect SCHAD. Briefly, ~100 mg of freshly harvested tissue (liver, kidney, and brain) was washed with PBS and homogenized in PBS plus 1% Triton. A total 15 μg of protein, including fresh isolated islets, was loaded in each lane of 10% SDS-PAGE mini-gels and after electrophoresis proteins were transferred to nitrocellulose membranes. A chicken polyclonal anti-SCHAD antibody (Abcam, Cambridge, MA), and a rabbit anti-actin antibody (Sigma) were used as the primary antibodies; a goat polyclonal anti-chicken IgY horseradish peroxidase conjugate (Abcam) and a donkey anti-rabbit IgG- Horseradish peroxidase conjugate (Amersham Biosciences) were used as the secondary antibodies. Membranes were blocked and incubated with antibody in 5% milk in PBS-Tris buffer and washed in PBS-Tris plus 0.02% Tween 20. Antibody-protein complexes were detected with the ECL reagent (Amersham Biosciences). As shown in Fig. 1 (*A–C*), *hadh* gene, *hadh* cDNA, and SCHAD protein were successfully deleted.

SCHAD and GDH Gene Expression—Total RNA were isolated from islets, liver, and kidney using the TRIzol (Invitrogen) method. For the reverse transcription reaction, a 40-μl PCR reaction efficiently converts 1.0 μg of total RNA to cDNA (Invitrogen). The sequences of primers were as indicated: for SCHAD-forward: CCA CCA GAC AAG ACC GAT TT; for SCHAD-reverse: TCA ATG AGG TAT GGC ACC AA; for GDH-forward: CTA TGG AGC TGG CCA AGA AG; for GDH-reverse: CCT ATG GTG CTG GCA TAG GT; for GAPDH-forward: AAC TTT GGC ATT GTG GAA GG; and for GAPDH-reverse: GGA TGC AGG GAT GAT GTT CT. Quantitative Real-Time PCR (Applied Biosystems SYBR Green Master Mix Kit) was carried out in low reaction volumes in 384-well plates using 7.5 μl of 2× SYBR Green master mix, 0.2 μl of primer (10 μM), 1 μl of cDNA, and water added to bring the final volume of 15 μl. Thermal cycle condition were: at 50 °C for 2 min, at 95 °C for 10min, followed by 40 cycles at 95 °C for 15 s and at 60 °C for 1 min. Experiments were performed with the 7900HT sequence detection system (Applied Biosystems). Islets mRNA level were calculated using GAPDH as standard and internal controls.

Islet Immunohistochemistry—8- to 12-week-old $hadh^{-/-}$ and $hadh^{+/+}$ male mice were anesthetized and transcardially perfused with 10 ml of saline, followed by 50 ml of fixative containing 4% paraformaldehyde and 0.125% glutaraldehyde. The slices of pancreas were treated with a mixture of 1% bovine serum albumin, 5% normal goat serum, and 0.3% Triton X-100 in 0.01 M phosphate buffer (PBS, pH 7.4) for 60 min at room temperature before incubation with a goat anti-glucagon antibody (1:500 in PBS, Santa Cruz Biotechnology) and guinea pig anti-insulin antibody (1:500 in PBS) for 90 min at room temperature and then overnight at 4 °C. The slices were subsequently incubated with Alexa Fluor 594-conjugated donkey anti-goat IgG (Molecular Probes) and Cy2-

conjugated donkey anti-guinea pig IgG (Jackson Laboratories). Both secondary antibodies were diluted at 1:250 in PBS, containing Hoechst (a nuclear dye). Confocal images were acquired under an Olympus Fluoview 1000 System (Olympus) at a step of 0.5 μm on the Z-axis. Consistent confocal settings were optimized and remained unchanged during the imaging of both *hadh*$^{-/-}$ and *hadh*$^{+/+}$ slices.

Oral Amino Acid Tolerance Test, Oral Glucose Tolerance Test, and Insulin Tolerance Test—All experiments were carried out in male mice, aged 10–12 weeks. Oral amino acid tolerance tests were performed on 2-h fasted mice using an amino acid mixture (composition described previously (7)), which was administered via oral gavage with a dose of 1.5 g/kg of body weight. Oral glucose tolerance tests were performed on 24-h fasted mice using 2g/kg of glucose via oral gavage. Insulin tolerance tests were performed on 2-h fasted mice using human insulin (1 unit/kg, intraperitoneally). Blood samples were taken from the tail at the indicated times. Plasma glucose concentrations were measured using a Freestyle flash glucose meter, and insulin was measured using an ELISA kit (ALPCO).

Metabolite Assays—Acylcarnitine species were analyzed in mouse plasma as butylated derivatives using flow injection tandem mass spectrometry that has been validated for clinical use in humans (8). Data collection was performed in a multiple reaction monitoring system using the parent ions of the fragment with *m/z* 85 as reference. Quantitation of acylcarnitine was achieved using a series of stable-isotope-labeled internal standards (8). Urine organic acids were analyzed by gas chromatography/mass spectrometry as trimethylsilyl derivatives with full scan data collection for positive peak identification. This assay is also validated for clinical use in humans (9). Plasma 3-hydroxy fatty acids were measured using stable isotope dilution gas chromatography/mass spectrometry (10).

Mouse Islet Isolation, Insulin Secretion, and Cytosolic Ca^{2+} Measurements—Isolation of pancreatic islets, perifusion, and insulin assays were carried out as previously described (11). In brief, islets were isolated by collagenase digestion and cultured with 10 mM glucose in RPMI 1640 medium (Sigma) for 3–4 days. Islets were perifused in a Krebs-Ringer bicarbonate buffer with 0.25% BSA at a flow rate of 2 ml/min. Insulin was measured by radioimmunoassay. $[Ca^{2+}]_i$ was measured by dual wavelength fluorescence microscopy using a Zeiss AxioVision system as described previously (7).

ATP, ATP/ADP Ratio, and Intracellular Amino Acid Measurements—Batches of 100 isolated cultured islets were preincubated with Krebs-Ringer bicarbonate buffer for 60 min and then incubated with glucose-free buffer as basal; with glutamine/leucine (2/0.46 mM) in combination with or without additional 1.25 mM alanine and with 12 mM amino acid mixture (AAM) with or without 25 mM glucose and 25 mM glucose alone for another 60 min. Measurements of ATP, ATP/ADP ratio, intracellular amino acids, and insulin and glucagon release were described previously (12).

[U-^{14}C]Glutamine Oxidation—[U-^{14}C]glutamine (NEN-Life Science Products, UK) oxidation was measured in cultured islets as described previously (13, 14).

GDH and SCHAD Enzyme Activity—Tissue (freshly isolated islets, liver, and kidney) was homogenized in phosphate buffer (5 mM Na_2HPO_4, 5 mM K_2HPO_4, 1 mM EDTA, 1% Triton X-100, pH 7.4). GDH and SCHAD activities were assayed spectrophotometrically at 340 nm by monitoring oxidation of NADH (11, 15, 16) in a 384-well plate format in a 25-μl reaction volume using a SpectraMax M5 (Molecular Devices). Because of limited tissue, studies of islet GDH kinetics were carried out in the presence of either maximal (100 μM) or submaximal stimulatory (10 μM for K_m) concentrations of ADP. K_m and V_{max} for α-ketoglutarate were calculated by using GraphPad Prism. For His-SCHAD/GDH mixing experiments, the molar concentration of GDH in liver was estimated from the maximal ADP-stimulated activity, using bovine GDH (Sigma) as a standard. Different amounts of His-SCHAD were added to the homogenate prior to assays of GDH kinetics.

Immunoprecipitation by Anti-SCHAD Antibody—Fresh liver mitochondria from both *hadh*$^{+/+}$ and *hadh*$^{-/-}$ mice were isolated using a Mitochondria Isolation Kit (Qiagen). Sample sizes of 60 mg per preparation were found to be optimal. All steps were performed at 4 °C. Mitochondria pellets were lysed in PBS with 1% Triton, and the protein concentration was adjusted to 5 μg/μl. Immunoprecipitation was performed using the Seize Primary Mammalian Immunoprecipitation Kit (Pierce). Briefly, 100 μg of affinity-purified anti-SCHAD antibody (Abcam) was bound to AminoLink Plus Coupling Gel (200 μl of pre-washed 50% gel slurry). The antibody-coupled gel was thoroughly washed and divided into two columns. Mitochondrial extracts were mixed 1:1 with PBS to a volume of 400 μl (1 mg protein) and then added to the antibody-coupled gel. After incubation with gentle mixing for 16 h at 4 °C, the gel was washed with PBS-Tris buffer and the immunoprecipitated antigen was eluted in elution buffer. Western blot analysis was performed using a rabbit polyclonal anti-GDH antibody (Abcam).

His-SCHAD Pulldown Assay—Recombinant His-tagged SCHAD protein was expressed in *Escherichia coli* using the pET 20 (b+) expression vector containing a full-length mouse *hadh* cDNA and a C-terminal His Tag (Novagen). The His-tagged SCHAD protein was purified using Ni-His Columns (Novagen) by standard methods. Protein pulldown experiments were performed using an Aminolink Plus Immobilization Kit (Pierce). Briefly, His-tagged SCHAD protein was covalently cross-linked to the Aminolink agarose resin. Liver tissue (0.5 g wet weight) from *hadh*$^{+/+}$ and *hadh*$^{-/-}$ mice was homogenized using 20 volumes of mammalian protein extraction reagent (M-PER, Pierce) and centrifuged at 2000 $\times$ *g* for 10 min. The supernatant was mixed with an equal volume of M-PER binding buffer and incubated with the SCHAD-linked amino link resin at 4 °C overnight. The resin was centrifuged (2000 $\times$ *g*) after incubation and washed with (0.5 ml, M-PER) washing buffer, and bound proteins were eluted with 200 μl of M-PER elution buffer. Western blot analysis of the eluted proteins was performed, and the blot was probed with a polyclonal anti-GDH antibody.

Proteomic Analysis of Pulldown Proteins by Recombinant SCHAD Protein—Mass spectrometry analysis of the protein complexes from the pulldown assay using His-tagged SCHAD protein was performed at the protein core facility of the Depart-

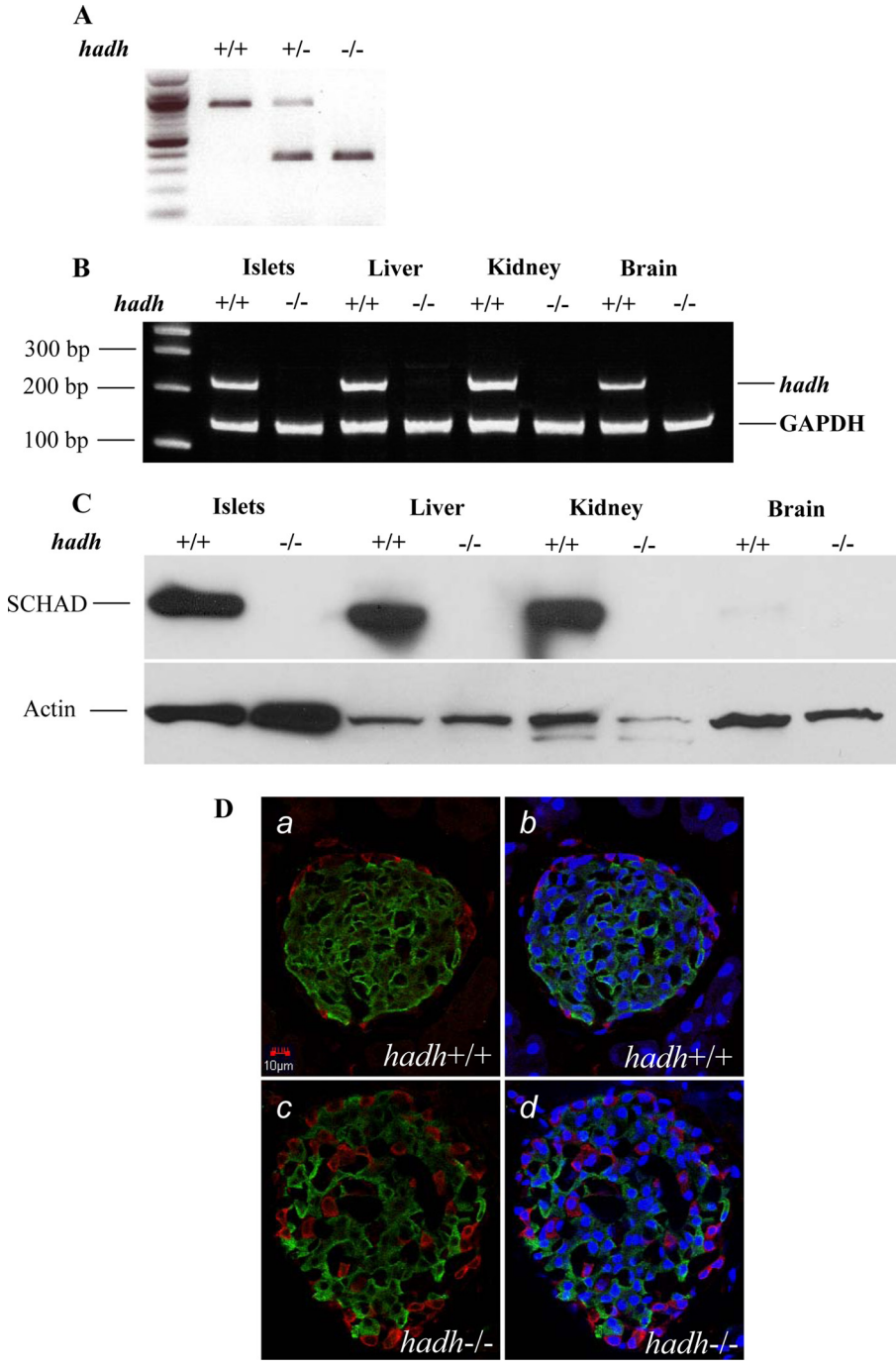

FIGURE 1. **Knock-out of *hadh* gene in mice and islet immunohistochemistry.** Genetic ablation of *hadh* was confirmed by PCR from mouse DNA (*A*). Analysis of mRNA expression by RT-PCR (*B*) and Western blot analysis of protein extracts (*C*) from multiple mouse tissues provided further evidence of *hadh* gene deletion. *D* shows islet immunohistochemistry, and islets from $hadh^{+/+}$ (*a* and *b*) and −/− (*c* and *d*) are shown. Insulin is stained *green*, glucagon is *red*, and nuclear is *blue*.

ment of Pathology & Laboratory Medicine at the University of Pennsylvania. The protein complex was digested with trypsin followed by tandem mass spectrometric analysis of the peptide sequences. Identified sequences were matched to the proteins using Scaffold protein identification software v 2.0.

Immunoprecipitation by Anti-GDH Antibody—200 μl of a 50% suspension of protein A beads (Invitrogen) and 200 μl of Rabbit anti-GDH antibody (Rockland) were incubated for 2 h at room temperature by gently mixing, then washed 5 times with 400 μl of PBS-T buffer. Islets from $hadh^{-/-}$ and $hadh^{+/+}$ mice were homogenized using PBS buffer plus 1% Triton. 1 mg (400 μl) of islets lysates protein was then incubated at 4 °C overnight with protein A beads bound with anti-GDH antibody. After washing 5 times with PBS-T buffer, the samples were eluted with elution buffer (Pierce). SCHAD protein was detected by Western blot using anti-SCHAD antibody.

Materials—All chemicals were from Sigma except as otherwise indicated.

Data Analysis—All the data are presented as mean ± S.E. Student *t* test was performed when two groups were compared. Repeated measures of analysis of variance were performed when multigroups were compared. Differences were considered significant for $p < 0.05$.

RESULTS

hadh Gene and SCHAD Protein Deletion—As shown in Fig. 1 (*A–C*), *hadh* gene, *hadh* cDNA, and SCHAD protein were successfully deleted in all tissues, including liver, kidney, brain, and isolated pancreatic islets.

In Vivo Metabolite Changes Resulting from SCHAD Deletion—As shown in Table 1, $hadh^{-/-}$ mice showed abnormalities of plasma and urinary metabolites similar to those found in children with SCHAD deficiency. In the fed state, there was a 4-fold elevation of plasma 3-hydroxybutyrylcarnitine in $hadh^{-/-}$ mice compared with controls, similar to values reported in children with SCHAD deficiency (2, 3). The remaining profile of acylcarnitines from C2 to C18 was indistinguishable from normal (data not shown). After 24 h of fasting, levels of 3-hydroxybutyrylcarnitine increased in control, but not in $hadh^{-/-}$ mice, although levels remained higher in $hadh^{-/-}$ mice. 24 h of fasting also resulted in increased plasma 3-hydroxy-fatty acids of C6 and C8 species in $hadh^{-/-}$ mice. 3-Hydroxy-fatty acids of chain lengths C10 to C18 were indistinguishable from normal (data not shown). Urine from $hadh^{-/-}$ mice had increased excretion of 3-hydroxyglutarate, which has been reported in affected SCHAD-deficient children, and also of glutaconic acid, which is an unstable metabolite

TABLE 1
Metabolites in hadh$^{-/-}$ mice

Metabolites	Conditions/Species	*hadh*$^{-/-}$	*hadh*$^{+/+}$
Plasma 3-OH-butyrylcarnitine (μM, $n = 3$)	Fed	0.61 ± 0.08[a]	0.16 ± 0.02
	24 h fasted	0.43 ± 0.08	0.27 ± 0.03
Plasma 3-OH-fatty acids (μM, $n = 6$, 24-h fasted)	C6	2.4 ± 0.4[a]	0.8 ± 0.1
	C8	0.6 ± 0.1[a]	0.3 ± 0.0
Urine organic acids (mmol/mol creatinine, 24-h fasted, $n = 3$)	3-Hydroxyglutarate	34 ± 8	ND[b]
	Glutaconate	34 ± 17	ND

[a] $p < 0.01$ *versus* *hadh*$^{+/+}$.
[b] ND, non-detectable.

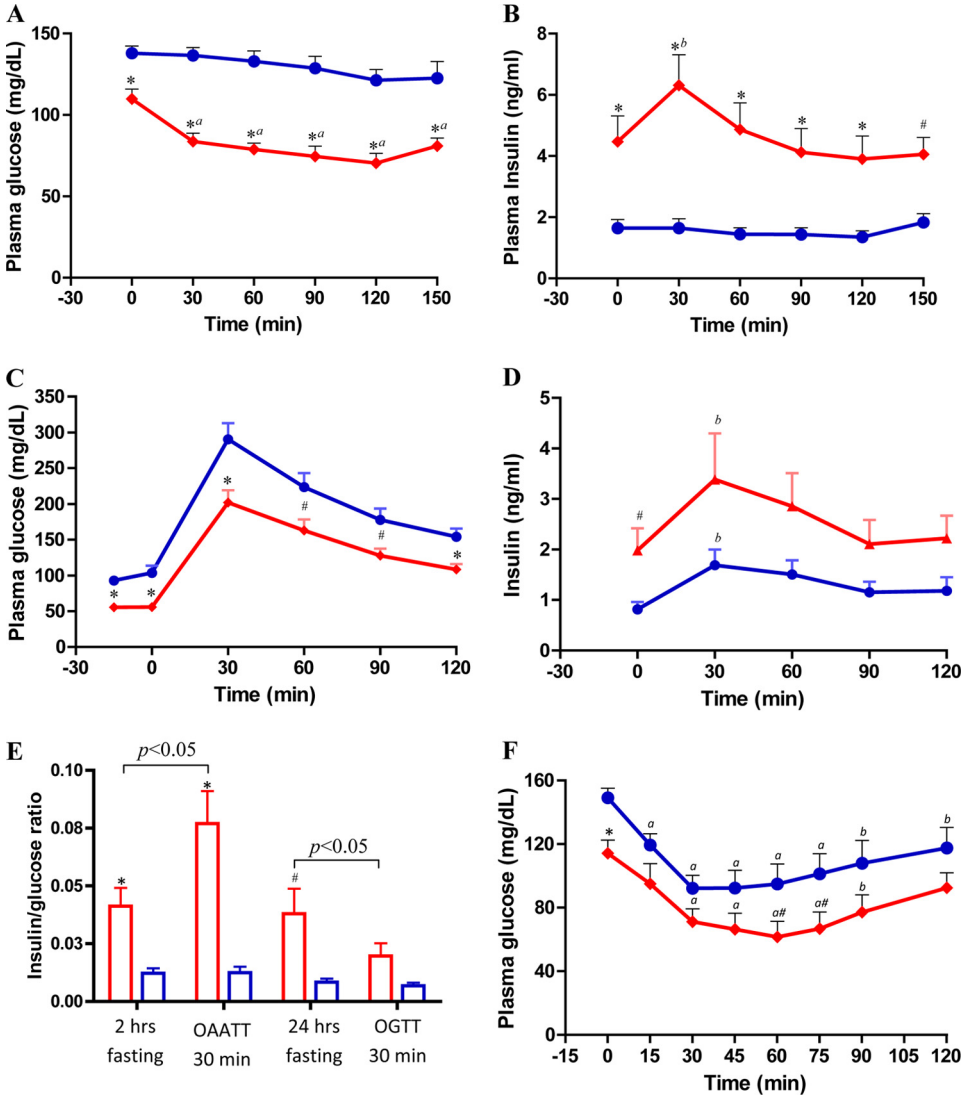

FIGURE 2. **Effect of *hadh* deletion on glucose homeostasis *in vivo*: oral amino acid and glucose tolerance test and insulin sensitivity.** *A* and *B*, plasma glucose and insulin responses to an oral mixture of amino acids in 2-h fasted *hadh*$^{-/-}$ (*diamonds*, *red*, $n = 16$) and *hadh*$^{+/+}$ (*circles*, *blue*, $n = 16$) mice. *C* and *D*, plasma glucose and insulin responses to oral glucose tolerance test in 24-h fasted *hadh*$^{-/-}$ (*diamonds*, *red*, $n = 19$) and *hadh*$^{+/+}$ (*circles*, *blue*, $n = 9$) mice. *E*, insulin/glucose ratio calculated base on 2- and 24-h fasted −/− (*red bar*) and +/+ mice (*blue bar*), and at the time of 30 min after either challenged by oral amino acid or glucose. *F*, insulin tolerance test in 2-h fasted *hadh*$^{-/-}$ and *hadh*$^{+/+}$ mice ($n = 12$ for both). Compared with +/+ mice; *, $p < 0.01$; #, $p < 0.05$; compared with time 0; *a*, $p < 0.01$; *b*, $p < 0.05$. Results are presented as means ± S.E.

derived from glutaconyl-CoA, an intermediate of glutaryl-CoA reduction. This has not been previously detected in affected children but is seen in some patients with glutaryl-CoA dehydrogenase deficiency (17).

Pancreatic histology in the *hadh*$^{-/-}$ mice showed abnormalities similar to that of SUR1 knock-out (SUR1$^{-/-}$) islets; *i.e.* glucagon-staining α-cells were distributed throughout the islet, rather than being restricted to the outer margin (Fig. 1*D*). Glucagon content was comparable in *hadh*$^{-/-}$ *versus* *hadh*$^{+/+}$ islets (2.6 ± 0.6 *versus* 2.4 ± 0.8 ng/μg islets protein, $n = 10$, $p > 0.05$).

Amino Acid, Glucose, and Insulin Sensitivity in Vivo—Because hypersensitivity to amino acid stimulation of insulin release has been reported to be part of the phenotype of children with SCHAD deficiency (6), we examined responses of hadh$^{-/-}$ mice to an amino acid challenge *in vivo*. As shown in Fig. 2, *A* and *B*, after 2 h of fasting, basal glucose was significantly lower and basal insulin significantly elevated in *hadh*$^{-/-}$ mice. Following oral amino acid stimulation, there were significant decreases in glucose and increases in plasma insulin in the *hadh*$^{-/-}$ mice, whereas there were no significant changes in glucose or insulin levels in control mice. This observation is consistent with the observation of protein-sensitive hypoglycemia in children with SCHAD deficiency.

As shown in Fig. 2*C*, *hadh*$^{-/-}$ mice also demonstrated lower plasma glucose levels than controls after 24-h fasting. An oral glucose tolerance test in these 24-h fasted mice demonstrated no difference in glycemic responses between knock-out and controls (areas under the curve using basal glucose level as baseline were similar: −/−: 10545 ± 1036 *versus* +/+: 12200 ± 1587, $p > 0.05$). The increases in plasma insulin following oral glucose (Fig. 2*D*) were also similar, despite the fact that fasting glucose levels in −/− mice were significantly lower and insulin levels were significantly higher than in controls (areas under the curve similar using basal level as baseline, −/−: 77 ± 22 *versus* +/+: 75 ± 21, $p > 0.05$).

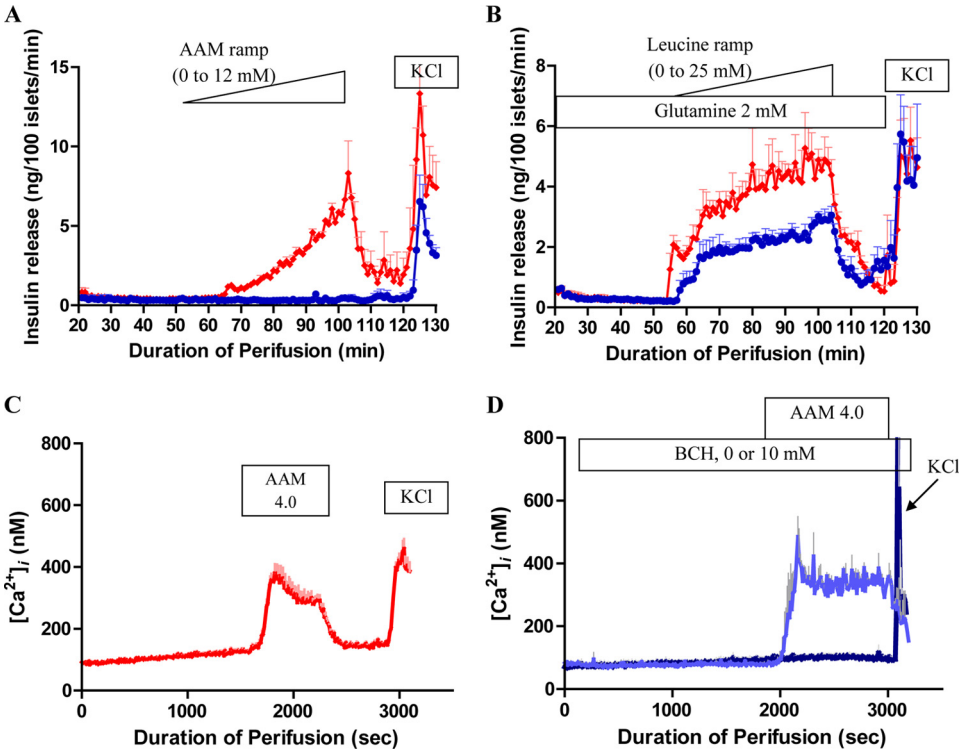

FIGURE 3. **Effect of *hadh* deletion on amino acid-stimulated insulin secretion and $[Ca^{2+}]_i$ changes in isolated islets.** *A* and *B*, isolated islets from *hadh*$^{-/-}$ (*diamonds*, *red*) and *hadh*$^{+/+}$ (*circles*, *blue*) mice were cultured with 10 mM glucose for 3 days and then perifused with an amino acid mixture ramp (0–12 mM, 0.24 mM/min, *A*) or a leucine ramp (0–25 mM, 0.5 mM/min, *B*) in the presence of 2 mM glutamine. Finally islets were exposed to 30 mM KCl. Results are presented as mean ± S.E. from three separate perifusions. *C* and *D*, $[Ca^{2+}]_i$ was continually measured by Fura-2 fluorescence in cultured islets in response to a 4.0 mM mixture of amino acids in *hadh*$^{-/-}$ (*C*) and *hadh*$^{+/+}$ islets (*D*, in the absence of 2-amino-2-norbornanecarboxylic acid, *dark blue line*, or the presence of 10 mM 2-amino-2-norbornanecarboxylic acid, *light blue line*). Results are presented as mean ± S.E. from 3–6 separate perifusions.

As shown in Fig. 2*E*, the insulin/glucose ratios in *hadh*$^{-/-}$ mice were significantly higher in both the 2-h and 24-h fasted conditions. After oral amino acid challenge, the elevated insulin/glucose ratio increased even further in −/− mice, but not in controls. In contrast, glucose administration partially corrected the inappropriately elevated insulin/glucose ratio in −/− mice. The degree of fasting hypoglycemia in *hadh*$^{-/-}$ mice was more severe than that of SUR1$^{-/-}$ mice, but not as severe as in RIP H545Y huGDH gain of function transgenic mice (12, 18). Female *hadh*$^{-/-}$ mice had fasting and non-fasting hypoglycemia similar to male mice (data not shown).

As shown in Fig. 2*F*, there was no evidence of increased insulin sensitivity in 2-h fasted *hadh*$^{-/-}$ compared with *hadh*$^{+/+}$ mice. The slopes of the decrease in glucose levels in the insulin tolerance test were similar (−/− *versus* +/+, −1.27 ± 0.02 *versus* −1.28 ± 0.02, $p > 0.05$). The knock-out mice had a faster recovery rate (slopes from 60 to 120 min were 0.49 ± 0.03 for −/− and 0.26 ± 0.02 for +/+, $p < 0.01$), indicating that the counter-regulatory hormone secretion in response to hypoglycemia was not impaired in *hadh*$^{-/-}$ mice.

Amino Acid-stimulated Insulin Secretion and Leucine-stimulated Insulin Secretion and Cytosolic Calcium ($[Ca^{2+}]_i$) Responses in Isolated Islets—To investigate the mechanism of insulin dysregulation and hypersensitivity to amino acids in *hadh*$^{-/-}$ mice, we first examined insulin responses of isolated cultured islets to stimulation by a mixture of amino acids. As shown in Fig. 3*A*, islets from *hadh*$^{-/-}$ mice showed dramatic sensitivity to ramp stimulation with an AAM, whereas both *hadh*$^{+/+}$ and *hadh*$^{+/-}$ islets (data not shown) had no response. The threshold for amino acid-stimulated insulin secretion in *hadh*$^{-/-}$ islets was 2.64 mM, which is less sensitive than we previously found in transgenic islets expressing the human H454Y GDH-activating mutation (1.68 mM) (12). As shown in Fig. 3*B*, in the presence of 2 mM glutamine, *hadh*$^{-/-}$ islets had a lower threshold (1.5 *versus* 3 mM) and increased maximum for leucine stimulation of insulin secretion compared with +/+ islets, suggesting an increased sensitivity of GDH to allosteric activation by leucine.

Hypersensitivity to amino acid-stimulated insulin secretion also occurs in the SUR$^{-/-}$ mouse model of hyperinsulinism, but not through leucine stimulation of GDH. Instead, it reflects a specific effect of glutamine to amplify insulin release in the presence of the elevated levels of cytosolic $[Ca^{2+}]_i$ resulting from the absence of K_{ATP} channel activity (7). Fig. 3*C* shows that, unlike SUR1$^{-/-}$ islets, *hadh*$^{-/-}$ islets had normal basal levels of cytosolic $[Ca^{2+}]_i$. However, the *hadh*$^{-/-}$ islets were very sensitive to stimulation of $[Ca^{2+}]_i$ by a mixture of amino acids (3.5 mM AAM plus 0.5 mM glutamine) (Fig. 3*C*); in control islets, in contrast, an AAM stimulated $[Ca^{2+}]_i$ to rise only when GDH had been activated by pre-exposure to 10 mM 2-amino-2-norbornanecarboxylic acid, a non-metabolizable leucine analogue (Fig. 3*D*).

The Role of Leucine, Glutamine, and Alanine on Insulin Secretion—The above data suggested that increased sensitivity to leucine and amino acid-stimulated insulin secretion in *hadh*$^{-/-}$ islets involved activation of GDH. As shown in Fig. 4*A*, [U-^{14}C]glutamine oxidation was increased 2-fold in *hadh*$^{-/-}$ islets, providing further evidence of increased GDH activity. However, *hadh*$^{-/-}$ islets showed no insulin response to stimulation with glutamine alone (data not shown). This differed from the brisk response to glutamine we previously observed in the mouse model of GDH hyperinsulinism using transgenic islets expressing the H454Y huGDH-activating mutation (12). To investigate why the complete amino acid mixture was more potent than glutamine alone to stimulate insulin secretion in *hadh*$^{-/-}$ islets, we performed further experiments with combinations of individual amino acids. As shown in Fig. 4*B*, when glutamine was removed from the total mixture of amino acids, insulin secretion was decreased by 90% in *hadh*$^{-/-}$ islets, indicating that glutaminolysis played an

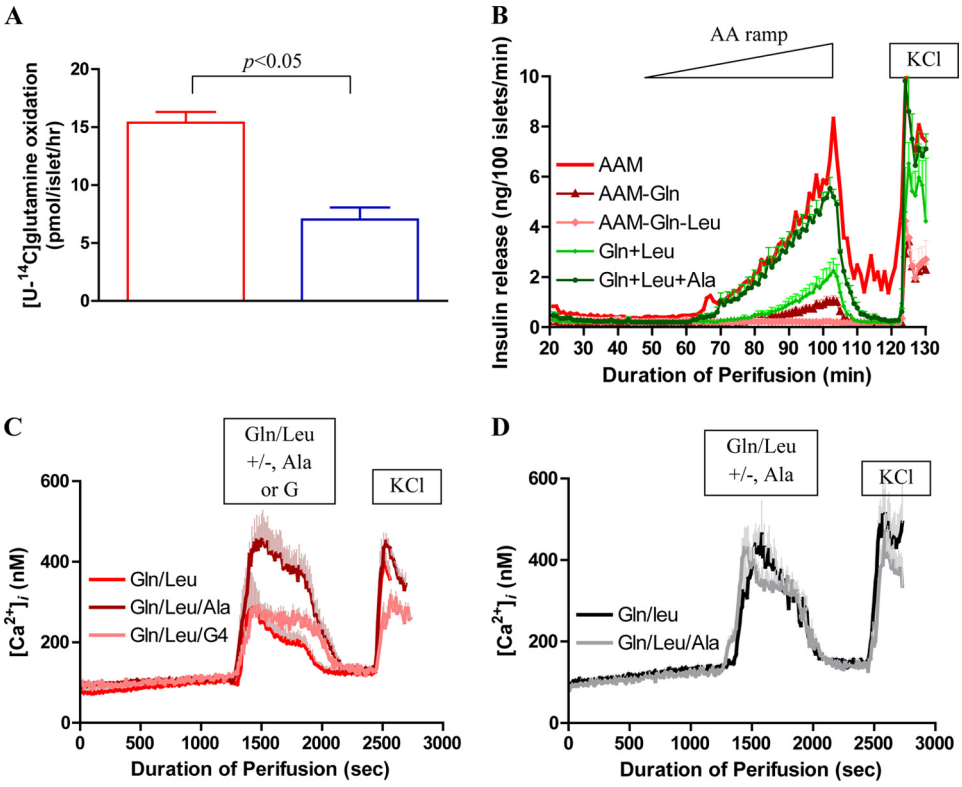

FIGURE 4. **[U-^{14}C]glutamine oxidation and the effect of leucine/glutamine/alanine on insulin secretion and $[Ca^{2+}]_i$.** *A*, [U-^{14}C]glutamine oxidation (2 mM) was measured in isolated cultured islets from *hadh*$^{-/-}$ (*red bar*) and *hadh*$^{+/+}$ (*blue bar*) mice (mean ± S.E., $n = 5$). *B*, isolated cultured islets from *hadh*$^{-/-}$ mice were perifused with different combinations of amino acids as indicated in the *panel* (results are presented as mean ± S.E. from three separate perifusions). *C*, $[Ca^{2+}]_i$ changes in response to glutamine/leucine (2 mM/0.46 mM) stimulation in the presence (*dark red line*) or absence (*red line*) of 1.25 mM alanine or 4 mM glucose (*pink line*) were measured in *hadh*$^{-/-}$ islets (mean ± S.E., $n = 4$). *D*, experiments similar to those in *C* were performed in islets from H454Y huGDH transgenic mice in response to glutamine/leucine along (*gray line*) or with additional alanine (*black line*) (mean ± S.E., $n = 3$).

important role in the response to the amino acid mixture. When glutamine and leucine were both removed from the amino acid mixture, *hadh*$^{-/-}$ islets were completely unresponsive, indicating that GDH activation by leucine was essential to the release of insulin (Fig. 4*B*). The response to a ramp combining glutamine (2 mM) plus leucine (0.46 mM) in the same concentrations as in the amino acid mixture was only 40% of that previously observed with the complete amino acid mixture (Fig. 3*A*). With addition of alanine to the glutamine/leucine combination (maximum concentration, 1.25 mM), the insulin response became equal to that obtained with the complete 19-amino acid mixture, indicating that the other 16 amino acids did not contribution to insulin release. The additive effect of alanine could not be reproduced by addition of 1.25 mM methylpyruvate, monomethylsuccinate, α-ketoisocaproate, or acetylcarnitine (data not shown).

As shown in Fig. 4*C*, measurements of $[Ca^{2+}]_i$ in −/− islets indicated that addition of alanine (1.25 mM) also enhanced the calcium response to the combination of glutamine plus leucine (2 and 0.46 mM). This additive effect of alanine was not due to formation of additional glutamate for the GDH reaction via transamination, because increasing the glutamine concentration of the glutamine/leucine mixture by an additional 1.25 mM was not as effective as alanine (data not shown). The alanine effect was partially reproduced by addition of 4 mM glucose, which suggests that providing additional pyruvate from either glucose or alanine was potentiating glutamine oxidation. Addition of alanine to glutamine/leucine stimulation of H545Y huGDH transgenic islets (12) had no effect on $[Ca^{2+}]_i$ (Fig. 4*D*), suggesting that glutaminolysis is already maximal in these islets.

GSIS and $[Ca^{2+}]_i$ Responses—Because the *in vivo* data revealed no evidence of abnormal insulin responses to glucose stimulation in *hadh*$^{-/-}$ mice, we further examined glucose-stimulated insulin secretion (GSIS) in perifused islets. Unlike the hypersensitivity of −/− islets to amino acid-stimulated insulin secretion, there were no differences between *hadh*$^{-/-}$ and *hadh*$^{+/+}$ islets in response to a glucose ramp stimulation (Fig. 5*A*). Addition of a medium-chain fatty acid, 1 mM octanoate, potentiated GSIS equally in −/− and +/+ islets. Addition of a long-chain fatty acid, 0.25 mM palmitate, had a slight inhibitory effect on GSIS, that was identical in −/− and +/+ islets (Fig. 5*B*). As shown in Fig. 5*C*, *hadh*$^{-/-}$ and *hadh*$^{+/+}$ islets showed similar basal cytosolic calcium ($[Ca^{2+}]_i$). The $[Ca^{2+}]_i$ responses to 10 mM glucose stimulation after a short period of islet rundown were also similar. However, after prolonged rundown, *hadh*$^{-/-}$ islets demonstrated an absence of the normal transient dip in $[Ca^{2+}]_i$ (19), resulting in an earlier rise in $[Ca^{2+}]_i$ following glucose stimulation. These changes in $[Ca^{2+}]_i$ dynamics suggested that deletion of the SCHAD protein caused an increase in basal islet metabolism, albeit insufficient to have a major effect on GSIS.

Amino Acid and Glucose Metabolism and Amino Acid Profiles in hadh$^{-/-}$ *Isolated Islets*—To further examine the apparent activation of GDH activity in *hadh*$^{-/-}$ islets, we determined the effects of glucose and amino acids on intracellular amino acid levels and insulin responses in batch-incubated *hadh*$^{-/-}$ and *hadh*$^{+/+}$ islets. In the absence of glucose, basal islet ATP content was elevated, and there was a trend toward increased ATP/ADP ratio in −/− islets, consistent with an increase in basal amino acid oxidation as a result of GDH activation. Consistent with this observation, −/− islets had significantly lower aspartate and glutamate levels than controls under glucose-free conditions. This apparent increase in amino acid oxidation under basal conditions was insufficient to stimulate insulin release. A combination of glutamine and a low concentration of leucine stimulated insulin secretion in *hadh*$^{-/-}$ but not in control islets. Under this condition also, the *hadh*$^{-/-}$ islets had significantly lower levels of aspartate, and the sum of alanine,

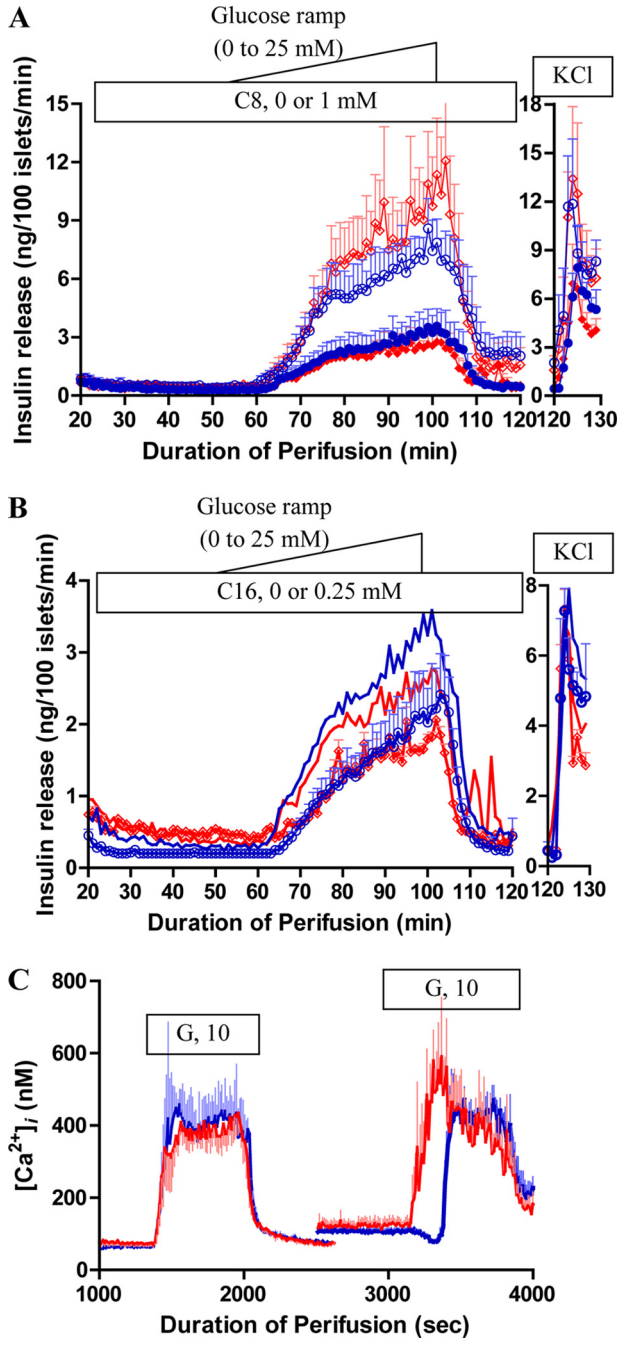

FIGURE 5. **Effect of *hadh* deletion on glucose-stimulated insulin secretion and $[Ca^{2+}]_i$.** Glucose stimulated insulin secretion in isolated cultured islets from $hadh^{-/-}$ (*diamonds*, *red*) and $hadh^{+/+}$ (*circles*, *blue*) mice, islets were perifused with a glucose ramp (0 to 25 mM, 0.5 mM/min) in the presence or absence of 1 mM octanoic acid (*A*, absence: *solid*, presence: *open*) or 0.25 mM palmitate (*B*, presence: *open*, absence: *blue* or *red line*). Finally, islets were exposed to 30 mM KCl. Results are presented as mean ± S.E. from three separate perifusions. *C*, cytosolic calcium, $[Ca^{2+}]_i$, was continually measured by Fura-2 fluorescence in cultured islets ($hadh^{-/-}$: *red line* and $hadh^{+/+}$: *blue line*) in response to 10 mM glucose after a short or long period of rundown. Results are presented as mean ± S.E. from four separate perifusions.

aspartate, glutamate, and glutamine was lower than in control islets. In $hadh^{-/-}$ islets, the addition of 1.25 mM alanine to the glutamine/leucine mixture further increased both insulin release and the ATP/ADP ratio to the same level as stimulation with 12 mM AAM. Under both conditions $hadh^{-/-}$ islets had lower alanine levels compared with controls, suggesting that alanine was being consumed to support a further increased rate of metabolism. This supports the suggestion above that the additive effect of alanine in $hadh^{-/-}$ islets may be to provide pyruvate to allow completion of glutamate oxidation in the tricarboxylic acid (TCA) cycle, thus generating a greater increase in the ATP/ADP ratio than that produced by incomplete oxidation of glutamate via trans-deamination into aspartate (see Fig. 7).

Stimulation with 25 mM glucose alone partially reversed the lower basal levels of glutamate and of the sum of alanine, aspartate, glutamate and glutamine in $hadh^{-/-}$ compared with control islets. Stimulation by a combination of glucose plus AAM eliminated the differences in insulin release and amino acid levels between $hadh^{-/-}$ and $hadh^{+/+}$ islets that were seen with stimulation by AAM alone. This inhibitory effect on glucose on islet amino acid metabolism can be explained by our previous observation that glucose metabolism inhibits GDH activity and flux through GDH (11–13).

Interestingly, $hadh^{-/-}$ islets had reduced levels of GABA compared with controls under all conditions. This is similar to our observations in $SUR1^{-/-}$ islets or control islets exposed to glyburide (20), in which reduced GABA levels correlate with decreased expression of glutamate decarboxylase. Glutamate decarboxylase gene expression was also found to be reduced in $hadh^{-/-}$ islets by both RT-PCR and real-time PCR analysis of islet mRNA (data not shown). As shown in Table 2, glucagon responses were similar in $hadh^{-/-}$ and control islets, being stimulated only by the complete mixture of amino acids.

Interaction of SCHAD and GDH Proteins—Because the functional analysis of pancreatic islets suggested an activation of GDH activity in islets lacking SCHAD protein, we examined the possibility of protein-protein interactions between the two enzymes, reported by Filling *et al.* (21), using liver mitochondria from $hadh^{-/-}$ and $hadh^{+/+}$ mice (Fig. 6, *A* and *B*). When anti-SCHAD antibody was used as bait (Fig. 6*A*), GDH was co-precipitated with SCHAD in $hadh^{+/+}$ mouse liver mitochondria, but not in −/− mice, consistent with a GDH-SCHAD protein complex in $hadh^{+/+}$ liver mitochondria. When purified His-tagged SCHAD protein was used as bait, GDH was co-precipitated in $hadh^{-/-}$ liver extracts (Fig. 6*B*, *right lane*), indicating that free GDH in $hadh^{-/-}$ liver mitochondria was readily available to form a protein complex with His-tagged SCHAD protein. In contrast, in $^{+/+}$ mice, the majority of GDH was associated with the endogenous SCHAD protein and unavailable to bind to His-tagged SCHAD (Fig. 6*B*, *center lane*).

Because SCHAD activity has been reported to be elevated in islets compared with liver (22), we measured SCHAD and GDH messenger RNA in $hadh^{+/+}$ islets and liver by real-time PCR. The ratio of SCHAD to GDH message was 5-fold higher in islets than in liver (15 ± 1.3 *versus* 2.7 ± 0.6, $n = 3$, $p < 0.01$). As shown in Fig. 6*C*, anti-GDH antibody was able to co-precipitate SCHAD in lysates of islets from $hadh^{+/+}$ mice, confirming that SCHAD associated with GDH in islets, as well as liver.

Mass spectrometric analysis of the $hadh^{-/-}$ liver mitochondrial extract from the pulldown assay illustrated in Fig. 6*B*, using His-tagged SCHAD protein as bait, confirmed the presence of two GDH peptide fragments. The amino acid sequences

TABLE 2
ATP/ADP ratio, ATP content, insulin release, glucagon release, and intracellular amino acid profile in response to different amino acids and glucose in hadh$^{-/-}$ and +/+ islets

	G 0 (n = 7)		Gln/Leu, G 0 (2/0.46 mM) (n = 4)		Gln/Leu/Ala, G 0 (2/0.46/1.25 mM) (n = 4)		AAM, G 0 (12 mM) (n = 4)		G 25 (n = 6)		AAM/G 25 (12 mM) (n = 6)	
	−/−	+/+	−/−	+/+	−/−	+/+	−/−	+/+	−/−	+/+	−/−	+/+
Insulin release (ng/μg protein/h)	2.6 ± 0.3	3.9 ± 0.7	11.5 ± 0.8^{a,b}	3.6 ± 1.5	17.8 ± 2.3^{a,b,c}	4.2 ± 1.7	23.4 ± 0.9^{a,b,d}	3.7 ± 1.1	40 ± 4^{a}	47 ± 10^{a}	59 ± 3^{e}	67 ± 3^{e}
Glucagon release (pg/μg protein/h)	13 ± 3	17 ± 4	29 ± 7	25 ± 12	21 ± 2	21 ± 8	53 ± 5^{a}	55 ± 9^{f}	10 ± 3	17 ± 5	23 ± 3	34 ± 8
ATP content (pmol/μg protein)	69 ± 5^{b}	44 ± 5	67 ± 5	52 ± 13	66 ± 7	60 ± 13	68 ± 6	59 ± 15	82 ± 4	76 ± 3^{a}	77 ± 4	76 ± 6^{a}
ATP/ADP ratio	4.3 ± 0.7	2.9 ± 0.3	4.2 ± 0.3	3.1 ± 0.6	7.4 ± 0.5^{b,d,f}	3.4 ± 0.3	6.7 ± 0.1^{b,d,f}	3.2 ± 0.6	8.8 ± 1.7	4.6 ± 0.7^{f}	8.0 ± 1.3^{f}	5.1 ± 0.9^{f}
Intracellular amino acid (nmol/mg protein)												
Alanine	4 ± 0	5 ± 1	5 ± 2	5 ± 1	42 ± 3^{g}	83 ± 15	31 ± 5^{g}	56 ± 6	13 ± 1^{a}	12 ± 1^{a}	44 ± 5	45 ± 5
Aspartate	9 ± 1^{b}	24 ± 2	58 ± 7^{g}	92 ± 8	60 ± 6^{g}	81 ± 3	55 ± 8	62 ± 8	13 ± 1^{a,b}	20 ± 2	29 ± 2^{e}	38 ± 4^{h}
Glutamate	17 ± 2^{b}	42 ± 2	59 ± 7	99 ± 15	72 ± 8	99 ± 13	68 ± 16	88 ± 5	50 ± 6^{a}	60 ± 6	81 ± 8^{h}	97 ± 8
Glutamine	3 ± 1	3 ± 1	40 ± 13	59 ± 15	44 ± 8	75 ± 20	38 ± 8	54 ± 3	3 ± 0	4 ± 0	50 ± 8^{h}	55 ± 8
Sum of four	31 ± 4^{b}	76 ± 9	161 ± 23^{g}	256 ± 25	217 ± 15^{g}	338 ± 48	192 ± 36	260 ± 22	78 ± 7^{a}	95 ± 9	236 ± 11	235 ± 21
γ-Aminobutyric acid	≤1	12 ± 2	≤1	11 ± 4	≤1	13 ± 6	≤1	14 ± 2	2 ± 0^{b}	6 ± 0^{f}	2 ± 0^{b}	7 ± 1^{h}
Leucine	≤2	≤2	9 ± 3	14 ± 3	10 ± 1	18 ± 4	9 ± 1	11 ± 1	≤2	≤2	8 ± 1	7 ± 0
Sum of Ser/Gly/Ile	58 ± 10	61 ± 11	67 ± 11	74 ± 1	60 ± 9	79 ± 5	216 ± 27	257 ± 25	65 ± 6	75 ± 8	226 ± 8	219 ± 18

[a] $p < 0.01$, *versus* G, 0 in same group.
[b] $p < 0.01$, *versus* +/+.
[c] $p < 0.05$, *versus* Gln/Leu in same group.
[d] $p < 0.01$, *versus* Gln/Leu in same group.
[e] $p < 0.01$, *versus* AAM in same group.
[f] $p < 0.05$, *versus* G, 0 in same group.
[g] $p < 0.05$, *versus* +/+.
[h] $p < 0.05$, *versus* AAM in same group.

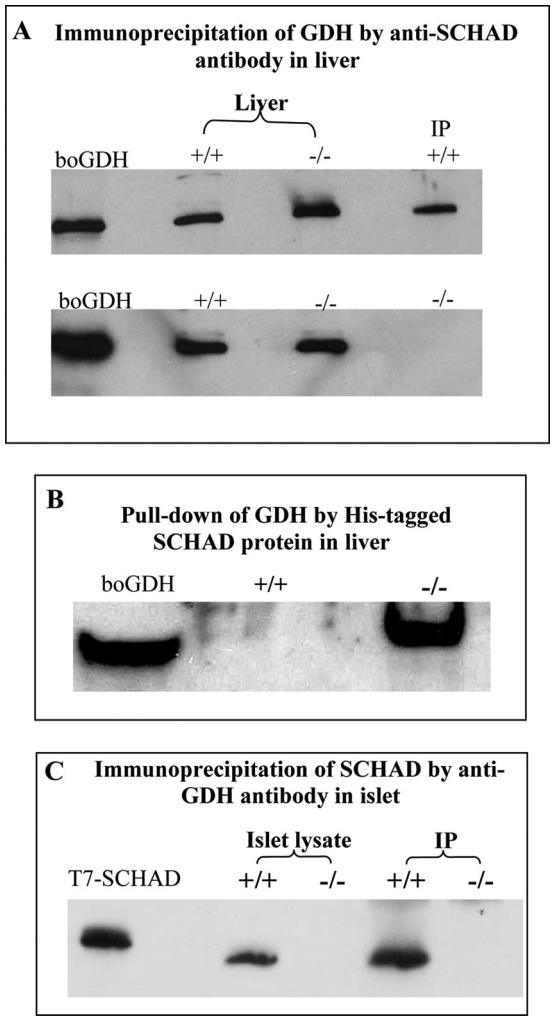

FIGURE 6. **Protein-protein interaction of SCHAD and GDH.** Immunoprecipitation was performed using extracts of isolated liver mitochondria (*A* and *B*) and islets (*C*) from *hadh*$^{-/-}$ and *hadh*$^{+/+}$ mice. *A*, Western blotting with anti-GDH antibody detected bovine GDH (*boGDH*, *left lane*) and mouse GDH in whole extracts of liver mitochondria from +/+ and −/− mice (*center two lanes*). Following precipitation of liver mitochondrial extracts with anti-SCHAD antibody as bait (*right lane*), GDH was only detected in the +/+ mice, but not in the −/− mice. *B* shows results of pulldown experiments using His-tagged SCHAD protein as bait. GDH was detected by anti-GDH Western blot in liver mitochondria extracts from *hadh*$^{-/-}$ mice (*right lane*) but not from *hadh*$^{+/+}$ mice (*middle lane*). *C*, immunoprecipitation of SCHAD using anti-GDH antibody as bait in isolated islets. Western blotting with anti-SCHAD antibody detected SCHAD protein in T7-SCHAD protein (*left lane*) and +/+ islets lysate as controls. SCHAD was also detected from +/+ islets after immunoprecipitation with anti-GDH, but not in −/− islets. All studies were repeated three to six times and showed similar results.

of these two peptides were (K)IIAEGANGPTTPEADKIFLER(N) and (K)YNLGLDLR(T). Interestingly, GDH was not the only protein in liver mitochondria from *hadh*$^{-/-}$ mice that was pulled down by His-tagged SCHAD. Mass spectrometry also revealed the presence of peptides from several other mitochondrial proteins, including carbamoyl phosphate synthetase-1 and 3-hydroxy-3-methylglutaryl-CoA lyase. The physiological roles of these proteins are liver-specific and are the subject of further investigation.

Islet GDH Enzyme Kinetics—To determine whether the absence of SCHAD protein altered GDH enzyme activity, we examined GDH and SCHAD activities in homogenates of islets,

TABLE 3
GDH enzyme kinetics and SCHAD activity in hadh$^{-/-}$ and +/+ mice
Data are mean ± S.E.

	Islets		Liver		Kidney	
	+/+	−/−	+/+	−/−	+/+	−/−
GDH activity (nmol/mg protein/min)						
Basal ($n = 4$)	28 ± 4	25 ± 1	214 ± 11[a]	193 ± 3[a]	83 ± 4[a,b]	96 ± 6[a,b]
Maximum (100 μM ADP, $n = 4$)	88 ± 8	84 ± 2	290 ± 13[a]	304 ± 11[a]	124 ± 10[a,b]	136 ± 8[a,b]
ADP stimulation (ED_{50}: μM, $n = 4$)	8 ± 2	13 ± 3	13 ± 1	15 ± 1	8 ± 2	9 ± 2
GTP inhibition[c] (ED_{50}: nM, $n = 4$)	309 ± 17	280 ± 28	30 ± 2	29 ± 2	44 ± 1	37 ± 1
K_m for α-KG[d] (μM, $n = 4$)	107 ± 8	63 ± 4[e]	124 ± 15	128 ± 15	74 ± 14	70 ± 13
SCHAD activity (nmo/mg protein/min, $n = 4$)	216 ± 7	ND[f]	127 ± 5[a]	ND	157 ± 16[a]	ND

[a] $p < 0.01$, *versus* islets in same group (−/− or +/+).
[b] $p < 0.01$, *versus* liver in same group.
[c] For islets, in the presence of 100 μM ADP.
[d] For islets, in the presence of 10 μM ADP.
[e] $p < 0.05$, *versus* +/+.
[f] ND, not detectable.

TABLE 4
Effect of His-SCHAD protein on GDH kinetics in hadh$^{-/-}$ liver

Molar ratio of His-SCHAD (dimmers) to GDH (hexamers) ($n = 6$)	K_m for α-ketoglutarate	V_{max}	Enzyme efficiency
	μM	*nmol/mg protein/min*	V_{max}/K_m
0	136 ± 15	340 ± 12	2.6 ± 0.3
0.3 ± 0.0	149 ± 22	350 ± 12	2.5 ± 0.3
1.2 ± 0.1	152 ± 13	318 ± 14	2.2 ± 0.3
3.1 ± 0.2	381 ± 25[a]	374 ± 22	1.0 ± 0.1[a]

[a] $p < 0.01$, *versus* no SCHAD (0).

liver, and kidney. As shown in Table 3, the ratio of SCHAD to GDH activities was markedly higher in islets compared with liver or kidney in *hadh*$^{+/+}$ mice. As we had previously observed, latent GDH activity (maximum minus basal activity) was greater in islets compared with liver and kidney implying the presence of some inhibitory effect, but this was similar in *hadh*$^{-/-}$ and *hadh*$^{+/+}$ islets. The ED_{50} values for allosteric inhibitors (GTP) and activators (ADP) were similar between −/− and +/+ mice in all three tissues. However, under conditions of submaximal stimulation with 10 μM ADP, the K_m for α-ketoglutarate was reduced in *hadh*$^{-/-}$ islets, but was not changed in liver or kidney. This reduced K_m for α-ketoglutarate in *hadh*$^{-/-}$ islets resulted in a 50% increase of enzyme efficiency as indicated by the ratio of V_{max} to K_m (0.4 ± 0.04 *versus* 0.6 ± 0.05, $p < 0.05$, $n = 4$). In contrast, the K_m for the second GDH substrate, ammonia, was unchanged in *hadh*$^{-/-}$ islets (data not shown). Islet GDH kinetics in the reverse, oxidative deamination, direction could not be measured, because, as expected, the reaction velocity was very low.

The increased affinity of GDH for α-ketoglutarate in *hadh*$^{-/-}$ islets was confirmed by adding back His-SCHAD protein to liver homogenate from −/− mice. As shown in Table 4, increasing the His-SCHAD/GDH molar ratio (SCHAD dimmers to GDH hexamers) to 3.1 reduced the affinity of GDH for α-ketoglutarate by 2.8-fold. Because the V_{max} remained unchanged, the addition of SCHAD protein to *hadh*$^{-/-}$ liver homogenate resulted in a 2.6-fold decrease in GDH enzyme efficiency. Similar results were also observed in mixing experiments using His-SCHAD and bovine GDH (data not shown). As shown in Table 4, intermediate elevations of the SCHAD/GDH molar ratio did not affect the K_m for α-ketoglutarate. This may explain why the inhibitory effect of SCHAD on GDH was only found in islets, but not in kidney and liver, because islets contained the highest ratio of SCHAD to GDH in both gene expression and enzyme activity.

DISCUSSION

These studies of mice with disruption of the SCHAD (*hadh*) gene demonstrate that they have a dysregulation of insulin secretion similar to the phenotype of hyperinsulinemic hypoglycemia reported in children with recessive inactivating mutations of *HADH* (also known as *HAD1*). *In vivo*, *hadh*$^{-/-}$ mice had reduced plasma glucose, increased plasma 3-hydroxybutyrylcarnitine, and increased urinary 3-hydroxyglutarate, consistent with observations in affected children. *In vitro* studies of isolated islets from *hadh*$^{-/-}$ mice showed increased sensitivity to amino acid-stimulated insulin secretion, indicating an activation of the glutaminolysis pathway through GDH to generate ATP and trigger release of insulin. Immunoprecipitation experiments demonstrated binding of SCHAD to GDH, and enzyme kinetic studies in islet homogenates showed that absence of SCHAD increases the enzymatic efficiency of GDH. These findings indicate that hyperinsulinism in SCHAD-deficient mice is caused by loss of a "moonlighting" function of the SCHAD protein, which normally provides a direct inhibitory effect on GDH enzymatic activity in pancreatic β-cells (Fig. 7).

A relationship between SCHAD deficiency and dysregulation of insulin secretion is clear in both humans and in mice. A total of five families has been reported with hyperinsulinism associated with SCHAD deficiency, and we are aware of three additional unpublished cases (2–4, 23). All of these cases had recessive mutations identified, and most appear to be associated with the absence of SCHAD protein, as well as enzymatic activity. It should be noted that other possible cases of SCHAD deficiency have been reported that did not have hyperinsulinism. In some, low SCHAD enzymatic activity was found in tissues, but none had mutations of the *HADH1* gene (24–26). One reported case with partial enzyme deficiency was compound heterozygous for *HADH1* missense mutations; in this case, the mutant protein was expressed in normal amounts, and the child did not appear to have hyperinsulinism (27). Kapoor *et al.* recently described protein-sensitive hypoglycemia in three cases of SCHAD deficiency with hyperinsulinism (6). This observation agrees with our finding of increased sensitivity to amino acid-stimulated insulin secretion *in vivo* and in isolated

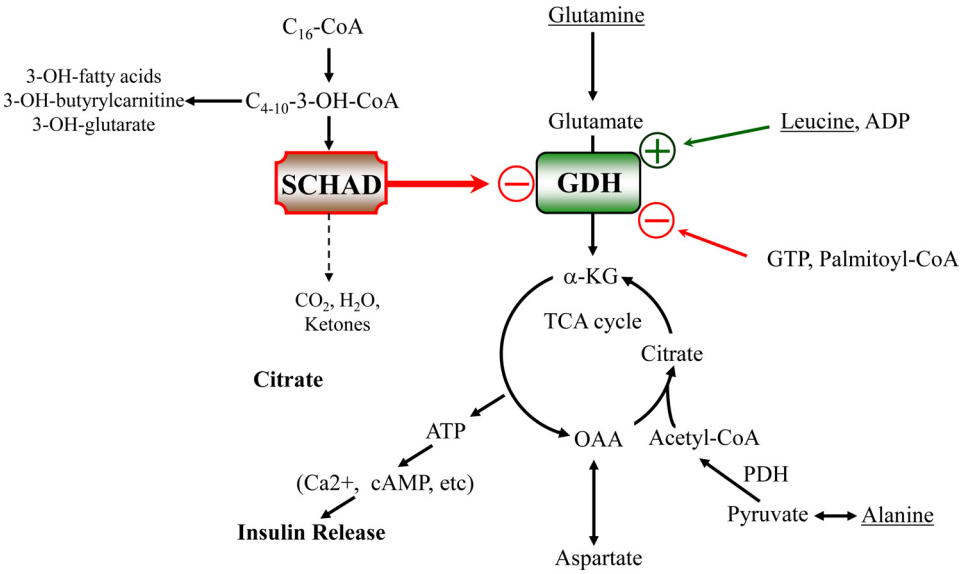

FIGURE 7. **Mechanism of insulin dysregulation in SCHAD deficiency.** In SCHAD-deficient islets, the loss of an inhibitory protein-protein interaction of SCHAD on GDH leads to an increase in the sensitivity of the GDH reaction to allosteric activation by leucine. Stimulation of islets by glutamine plus leucine *in vitro* produces a submaximal insulin response compared with stimulation with a complete physiological mixture of amino acids, because glutamate trans-deamination to aspartate uses only part of the TCA cycle to generate ATP as a trigger for insulin release. Addition of alanine to stimulation by glutamine plus leucine produces a greater release of insulin, equal to that of a mixture of amino acids, because the TCA cycle can be completed to generate a greater ATP response (18 *versus* 9 mol of ATP per mol of glutamate oxidized). *GDH*, glutamate dehydrogenase; *SCHAD*, short-chain 3-hydroxyacyl-CoA dehydrogenase; *α-KG*, α-ketoglutarate; *OAA*, oxaloacetate; and *TCA*, tricarboxylic acid.

islets from hadh$^{-/-}$ mice (6). Two of Kapoor's cases had mutations compatible with complete absence of SCHAD protein. The third case with protein-sensitive hyperinsulinism had a homozygous missense mutation with only a 50% reduction in enzyme activity and no abnormal fatty acid metabolites; it is possible that this amino acid change has little effect on enzymatic activity but interferes with the effect of the protein on GDH regulation.

SCHAD deficiency also appears to play a role in the hyperinsulinism associated with islet-specific knock-out of the FOXa2 transcription factor (28). Islets from these mice have reduced expression of both SCHAD and Kir6.2, one of the genes associated with the K_{ATP} channel form of hyperinsulinism. This combined deficiency causes a more severe hypoglycemic phenotype than deficiency of K_{ATP} alone, consistent with SCHAD deficiency having an independent role in causing hyperinsulinism. Attempts to identify the mechanism of hyperinsulinism in SCHAD deficiency using RNA interference to suppress enzyme expression have yielded inconsistent results. Our colleagues, Hardy *et al.*, found increases in basal, but not in glucose-stimulated insulin release when *hadh* was suppressed by RNA interference in INS 832/13 cells and in isolated mouse islets (29); the increased insulin release was not inhibited by diazoxide in the cells that were knocked down, suggesting a K_{ATP}-channel-independent mechanism. In contrast, Pipeleers and colleagues (22) reported that knock-down of *hadh* did not affect basal secretion, but increased insulin responses to GSIS and to depolarization with KCl in both INS cells and in rat islet cells; they suggested that an amplifying effect on GSIS of fatty acyl-CoAs proximal to the SCHAD step was responsible for hyperinsulinism in SCHAD deficiency. In contrast to both of these reports, the present findings in the SCHAD knock-out mouse did not show changes in GSIS, and neither of these knockdown studies addressed the protein sensitivity in SCHAD deficiency, which has recently been recognized to be an important feature of the disorder in children (6). The reasons for the different findings in the two studies with SCHAD knockdown are not clear, but an important factor may be the fact that both achieved only a partial, 50–80% reduction of SCHAD. Based on the reported cases of SCHAD deficiency associated with hyperinsulinism, this is likely insufficient to reproduce the hyperinsulinism phenotype. In a child with missense SCHAD mutations that reduced enzyme activity to 10–20% of normal (similar to the residual SCHAD expression reported in the knockdown experiments), there was no evidence of hyperinsulinism (27).

The present experiments suggest that the mechanism of insulin dysregulation associated with SCHAD deficiency is similar to that seen in children with activating mutations of GDH (30, 31). These mutations impair allosteric inhibition of GDH by GTP, thus leading to increased oxidation of glutamate and insulin release. Affected patients have increased sensitivity to activation of GDH by leucine, which is manifested clinically by hypoglycemia in response to ingestion of protein meals (32, 33). These patients also have persistent hyperammonemia, possibly due to the activation of GDH enzyme activity in the liver or kidney (34). Hyperammonemia is not a feature of SCHAD deficiency, perhaps because the activation of GDH may be limited to islets and also appears to be less severe than in GDH activating mutations.

Isolated *hadh*$^{-/-}$ islets demonstrate many similarities to those of islets expressing the H454Y-activating mutation of GDH. Islets from both mouse models release insulin in response to a physiological mixture of amino acids. Both show increased basal rates of glutaminolysis and a reduced threshold for leucine stimulation of insulin release, although the threshold in *hadh*$^{-/-}$ islets is intermediate between control and GDH transgenic islets (12). Unlike GDH transgenic islets, *hadh*$^{-/-}$ islets failed to release insulin in response to glutamine alone, but required the presence of leucine at concentrations that are not stimulatory in control islets. For maximum insulin response, islets from *hadh*$^{-/-}$ mice required exposure to alanine, glutamine, and leucine. The effect of alanine addition may be attributed to its contribution via acetyl-CoA formation to stimulate ATP production from the oxidation of glutamate in the tricarboxylic acid cycle (20) (see Fig. 7). These observations suggest that the degree of activation of GDH in *hadh*$^{-/-}$ is lower than in islets expressing the activating H454Y GDH; this

may account for the somewhat milder hypoglycemia of *hadh*$^{-/-}$ mice compared with the GDH transgenic mouse.

We did not observe any abnormalities in the responses of islets from SCHAD-deficient mice to the addition of fatty acids, including medium-chain fatty acids, which are substrates for the action of SCHAD. Octanoate potentiated the effect of amino acids on the stimulation of insulin secretion in *hadh*$^{-/-}$ islets, but this was not different from its effect on GSIS in both control and −/− islets. The failure to observe a specific effect of fatty acids on insulin secretion in *hadh*$^{-/-}$ islets indicates that the hyperinsulinism is not the result of accumulation of fatty acid intermediates. It is also consistent with the fact that other genetic defects of mitochondrial fatty acid beta-oxidation do not cause hyperinsulinism (5).

Measurements of cytosolic calcium responses to stimuli confirmed that the hyper-responsiveness of *hadh*$^{-/-}$ islets was specific to amino acid stimulation. Basal calcium concentrations and basal insulin secretion were normal in *hadh*$^{-/-}$ islets. This contrasts with islets from SUR1$^{-/-}$ mice, which serve as a model for the recessive form of hyperinsulinism due to inactivating mutations of the β-cell K_{ATP} channel. SUR1$^{-/-}$ islets lacking K_{ATP} channel activity are constitutively depolarized and have elevated basal concentrations of cytosolic calcium (7). In addition, patients with K_{ATP} channel inactivation are unresponsive to treatment with diazoxide, a K_{ATP} channel agonist, whereas patients with SCHAD deficiency respond well to diazoxide (2, 3, 6, 23). Thus, the hyperinsulinism associated with SCHAD deficiency is not due to abnormalities of the K_{ATP} channel. Cytosolic calcium responses to glucose stimulation showed subtle differences in *hadh*$^{-/-}$ islets (Fig. 5), which probably reflect increased metabolism of intracellular amino acids via GDH in the basal state (see also Table 2).

Our findings suggest that GDH activation in SCHAD deficiency is due to the loss of a direct protein-protein interaction between the two enzymes. This was demonstrated by both immunoprecipitation and protein pull-down experiments, confirming and extending observations recently reported by Filling *et al.* (21). That SCHAD may have a regulatory effect on GDH via this protein-protein interaction could not have previously been anticipated. As noted above, with the possible exception of one of the cases described by Kapoor (6), it appears that cases of SCHAD deficiency without hyperinsulinism express normal amounts of enzyme protein, whereas cases associated with hyperinsulinism lack SCHAD protein (including an unpublished case we have recently identified). This phenomenon, in which a protein has additional functions in other pathways, has been termed moonlighting protein effects (35). As in the present experiments, mass spectrometry has been useful in detecting such interactions (35). The pulldown experiments identified additional proteins that complex with SCHAD and GDH, including enzymes related to ureagenesis and ketogenesis, which might form a larger regulatory network. For example, although not detected in our SCHAD pulldown assays, SIRT4, one of the sirtuin enzymes involved in calorie-restriction longevity, has been reported to associate with GDH and inhibit its activity by ADP ribosylation (36).

Our experiments indicate that SCHAD reduces the affinity of GDH for α-ketoglutarate, but for not ammonia, suggesting that the presence of SCHAD affects binding of the carboxyl end of the substrate in the catalytic site. The effect was limited to islet GDH, perhaps reflecting the high levels of SCHAD (22) and, especially, the high ratio of SCHAD to GDH in this tissue (Table 3). It is interesting to speculate that the inhibitory effect of SCHAD on GDH might be part of a mechanism for reciprocal control of fatty acid and amino acid oxidation. Further work is clearly needed to define the details of how SCHAD modifies GDH activity, especially in islets.

In summary, the results of our studies of insulin dysregulation in *hadh*$^{-/-}$ mice provide an explanation for the hyperinsulinemic hypoglycemia reported in children with SCHAD deficiency. These mice display amino acid sensitive hypoglycemia *in vivo*. Their islets have abnormal sensitivity to amino acid stimulation of insulin secretion and demonstrate evidence of increased GDH activity, similar to islets expressing activating mutations of GDH. The activation of GDH appears to be related to a loss of a regulatory protein-protein interaction between GDH and SCHAD.

REFERENCES

1. De León, D. D., and Stanley, C. A. (2007) *Nat. Clin. Pract. Endocrinol. Metab.* **3,** 57–68
2. Hussain, K., Clayton, P. T., Krywawych, S., Chatziandreou, I., Mills, P., Ginbey, D. W., Geboers, A. J., Berger, R., van den Berg, I. E., and Eaton, S. (2005) *J. Pediatr.* **146,** 706–708
3. Molven, A., Matre, G. E., Duran, M., Wanders, R. J., Rishaug, U., Njølstad, P. R., Jellum, E., and Søvik, O. (2004) *Diabetes* **53,** 221–227
4. Jackson, S., Bartlett, K., Land, J., Moxon, E. R., Pollitt, R. J., Leonard, J. V., and Turnbull, D. M. (1991) *Pediatr. Res.* **29,** 406–411
5. Stanley, C. A., Bennett, M. J., and Mayatepek, E. (2006) *Disorders of Mitochondrial Fatty Acid Oxidation and Related Metabolic Pathyways*, 4th Ed., Springer, Heidelberg
6. Kapoor, R. R., James, C., Flanagan, S. E., Ellard, S., Eaton, S., and Hussain, K. (2009) *J Clin. Endocrinol. Metab.* **94,** 2221–2225
7. Li, C., Buettger, C., Kwagh, J., Matter, A., Daikhin, Y., Nissim, I. B., Collins, H. W., Yudkoff, M., Stanley, C. A., and Matschinsky, F. M. (2004) *J. Biol. Chem.* **279,** 13393–13401
8. Millington, D. S., Kodo, N., Norwood, D. L., and Roe, C. R. (1990) *J. Inherit Metab. Dis.* **13,** 321–324
9. Sweetman, L. (1991) in *Organic Acid Analysis* (Hommes, F. A., ed) pp. 143–176, Wiley-Liss, New York
10. Jones, P. M., Quinn, R., Fennessey, P. V., Tjoa, S., Goodman, S. I., Fiore, S., Burlina, A. B., Rinaldo, P., Boriack, R. L., and Bennett, M. J. (2000) *Clin. Chem.* **46,** 149–155
11. Li, C., Najafi, H., Daikhin, Y., Nissim, I. B., Collins, H. W., Yudkoff, M., Matschinsky, F. M., and Stanley, C. A. (2003) *J. Biol. Chem.* **278,** 2853–2858
12. Li, C., Matter, A., Kelly, A., Petty, T. J., Najafi, H., MacMullen, C., Daikhin, Y., Nissim, I., Lazarow, A., Kwagh, J., Collins, H. W., Hsu, B. Y., Nissim, I., Yudkoff, M., Matschinsky, F. M., and Stanley, C. A. (2006) *J. Biol. Chem.* **281,** 15064–15072
13. Gao, Z. Y., Li, G., Najafi, H., Wolf, B. A., and Matschinsky, F. M. (1999) *Diabetes* **48,** 1535–1542
14. Li, C., Allen, A., Kwagh, J., Doliba, N. M., Qin, W., Najafi, H., Collins, H. W., Matschinsky, F. M., Stanley, C. A., and Smith, T. J. (2006) *J. Biol. Chem.* **281,** 10214–10221
15. Passonneau, J. V., and Lowry, O. H. (1993) in *Enzymatic Analysis. A Practical Guide*, pp. 274–276, Humana Press, Totowa, NJ
16. Stanley, C. A., Fang, J., Kutyna, K., Hsu, B. Y., Ming, J. E., Glaser, B., and Poncz, M. (2000) *Diabetes* **49,** 667–673
17. Gregersen, N., and Brandt, N. J. (1979) *Pediatr. Res.* **13,** 977–981
18. De León, D. D., Li, C., Delson, M. I., Matschinsky, F. M., Stanley, C. A., and Stoffers, D. A. (2008) *J. Biol. Chem.* **283,** 25786–25793

19. Gylfe, E. (1988) *J. Biol. Chem.* **263,** 13750–13754
20. Li, C., Nissim, I., Chen, P., Buettger, C., Najafi, H., Daikhin, Y., Nissim, I., Collins, H. W., Yudkoff, M., Stanley, C. A., and Matschinsky, F. M. (2008) *J. Biol. Chem.* **283,** 17238–17249
21. Filling, C., Keller, B., Hirschberg, D., Marschall, H. U., Jörnvall, H., Bennett, M. J., and Oppermann, U. (2008) *Biochem. Biophys. Res. Commun.* **368,** 6–11
22. Martens, G. A., Vervoort, A., Van de Casteele, M., Stangé, G., Hellemans, K., Van Thi, H. V., Schuit, F., and Pipeleers, D. (2007) *J. Biol. Chem.* **282,** 21134–21144
23. Clayton, P. T., Eaton, S., Aynsley-Green, A., Edginton, M., Hussain, K., Krywawych, S., Datta, V., Malingre, H. E., Berger, R., and van den Berg, I. E. (2001) *J. Clin. Invest.* **108,** 457–465
24. Bennett, M. J., Spotswood, S. D., Ross, K. F., Comfort, S., Koonce, R., Boriack, R. L., IJlst, L., and Wanders, R. J. (1999) *Pediatr. Dev. Pathol.* **2,** 337–345
25. Bennett, M. J., Weinberger, M. J., Kobori, J. A., Rinaldo, P., and Burlina, A. B. (1996) *Pediatr. Res.* **39,** 185–188
26. Tein, I., De Vivo, D. C., Hale, D. E., Clarke, J. T., Zinman, H., Laxer, R., Shore, A., and DiMauro, S. (1991) *Ann. Neurol.* **30,** 415–419
27. Bennett, M. J., Russell, L. K., Tokunaga, C., Narayan, S. B., Tan, L., Seegmiller, A., Boriack, R. L., and Strauss, A. W. (2006) *Mol. Genet. Metab.* **89,** 74–79
28. Sund, N. J., Vatamaniuk, M. Z., Casey, M., Ang, S. L., Magnuson, M. A., Stoffers, D. A., Matschinsky, F. M., and Kaestner, K. H. (2001) *Genes Dev.* **15,** 1706–1715
29. Hardy, O. T., Hohmeier, H. E., Becker, T. C., Manduchi, E., Doliba, N. M., Gupta, R. K., White, P., Stoeckert, C. J., Jr., Matschinsky, F. M., Newgard, C. B., and Kaestner, K. H. (2007) *Mol. Endocrinol.* **21,** 765–773
30. Stanley, C. A. (2004) *Mol. Genet. Metab.* **81,** Suppl. 1, S45–S51
31. Stanley, C. A., Lieu, Y. K., Hsu, B. Y., Burlina, A. B., Greenberg, C. R., Hopwood, N. J., Perlman, K., Rich, B. H., Zammarchi, E., and Poncz, M. (1998) *N. Engl. J. Med.* **338,** 1352–1357
32. Hsu, B. Y., Kelly, A., Thornton, P. S., Greenberg, C. R., Dilling, L. A., and Stanley, C. A. (2001) *J. Pediatr.* **138,** 383–389
33. Kelly, A., Ng, D., Ferry, R. J., Jr., Grimberg, A., Koo-McCoy, S., Thornton, P. S., and Stanley, C. A. (2001) *J. Clin. Endocrinol. Metab.* **86,** 3724–3728
34. Treberg, J. R., Brosnan, M. E., Watford, M., and Brosnan, J. T. (2010) *Adv. Enzyme Regul.* **50,** 34–43
35. Jeffery, C. J. (2005) *Mass Spectrom. Rev.* **24,** 772–782
36. Haigis, M. C., Mostoslavsky, R., Haigis, K. M., Fahie, K., Christodoulou, D. C., Murphy, A. J., Valenzuela, D. M., Yancopoulos, G. D., Karow, M., Blander, G., Wolberger, C., Prolla, T. A., Weindruch, R., Alt, F. W., and Guarente, L. (2006) *Cell* **126,** 941–954